

REVISITING THE LEARNING OBJECTIVES OF VISION-LANGUAGE REWARD MODELS

Simon Roy^{*1}, Samuel Barbeau^{*2}, Giovanni Beltrame¹, Christian Desrosiers², Nicolas Thome³

¹ Polytechnique Montréal, ² École de Technologie Supérieure, ³ Sorbonne Université

ABSTRACT

Learning generalizable reward functions is a core challenge in embodied intelligence. Recent work leverages contrastive vision language models (VLMs) to obtain dense, domain-agnostic rewards without human supervision. These methods adapt VLMs into reward models through increasingly complex learning objectives, yet meaningful comparison remains difficult due to differences in training data, architectures, and evaluation settings. In this work, we isolate the impact of the learning objective by evaluating recent VLM-based reward models under a unified framework with identical backbones, finetuning data, and evaluation environments. Using Meta-World tasks, we assess modeling accuracy by measuring consistency with ground truth reward and correlation with expert progress. Remarkably, we show that a simple triplet loss outperforms state-of-the-art methods, suggesting that much of the improvements in recent approaches could be attributed to differences in data and architectures.

1 INTRODUCTION

The increasing momentum of embodied intelligence has motivated the study of generalizable reward models that do not rely on hand-crafted human supervision. Recent work leverages large vision-language models (VLMs) as general-purpose reward functions that measure progress through alignment between visual observations and language goals. Rocamonde et al. (2024) showed that CLIP (Radford et al., 2021) can be used as a zero-shot reward model for downstream policy learning, though it struggles with domain shift related to action specification and environmental dynamics. To mitigate this effect, many methods have turned to large-scale video demonstration datasets (Damen et al., 2018; Grauman et al., 2022) to finetune VLMs, enabling a better understanding of task-relevant behaviors. Nevertheless, the question of extracting meaningful signals of task progress from video demonstrations remains a central challenge to vision-language reward modeling. As a result, increasingly complex learning objectives have been proposed to generate more accurate rewards (Sermanet et al., 2018; Nair et al., 2022; Ma et al., 2023b;a; Karamcheti et al., 2023). However, most of these methods were pre-trained using different datasets and architectures, making it difficult to isolate the choice of learning objective from downstream performance. For instance, R3M (Nair et al., 2022) was pre-trained on Ego4D (Grauman et al., 2022) yet compares to methods pre-trained on ImageNet (Russakovsky et al., 2015; Parisi et al., 2022). LIV (Ma et al., 2023a) was initialized with CLIP weights and pre-trained on EpicKitchen (Nair et al., 2022) yet compares to methods utilizing a frozen BERT encoder Devlin et al. (2019) and vision encoder pre-trained on Ego4D from scratch (Nair et al., 2022).

In this work, we systematically compare objectives under a unified framework, holding the pre-trained model backbone, finetuning data, and downstream evaluation environments constant. This setup allows us to decouple the impact of the learning objectives from any other confounding factors. We assess model performance via two distinct benchmarks, evaluating consistency with ground truth reward and alignment with expert progress. While initially introduced as a minimal baseline for comparison with recent methods, our results show that a very simple triplet loss Schroff et al. (2015) can surpass current state-of-the-art learning objectives. More broadly, our findings indicate that simpler ranking-based learning objectives offer greater accuracy and robustness, suggesting

^{*}Equal contribution. Corresponding author: simon-7.roy@etud.polymtl.ca

that much of the apparent progress in recent methods could instead be due to differences in data and model architecture.

2 METHODOLOGY

State-of-the-art contrastive reward modeling approaches rely on combinations of learning objectives, either in their original form or adapted for alignment with language. For our experiments, we focus on a set of loss functions that can be used to reproduce many popular reward models.

TCN (Sermanet et al., 2018) reduces the embedding distance of images which are closer in time and increases the distance of images which are temporally further apart. Given an image encoder π_{img} , a sequence of images $\{I_t\}_{t=0}^k$, their corresponding encodings $z_t = \pi_{img}(I_t)$, batches of $[I_i, I_{j>i}, I_{k>j}]^{1:B}$ and a similarity function \mathcal{S} , TCN minimizes the following objective:

$$\mathcal{L}_{\text{TCN}} = -\frac{1}{B} \sum_{b \in B} \log \frac{e^{\mathcal{S}(z_i^b, z_j^b)}}{e^{\mathcal{S}(z_i^b, z_j^b)} + e^{\mathcal{S}(z_i^b, z_k^b)} + e^{\mathcal{S}(z_i^b, z_i^{\neq b})}} \quad (1)$$

We adapt \mathcal{L}_{TCN} to language by replacing $I_{k>j}$ with the language annotation for the given sequence. Inserting the language embedding $v = \pi_{\text{text}}(l)$ results in the following objective

$$\mathcal{L}_{\text{TCN}_{\text{text}}} = -\frac{1}{B} \sum_{b \in B} \log \frac{e^{\mathcal{S}(z_{j>i}^b, v^b)}}{e^{\mathcal{S}(z_{j>i}^b, v^b)} + e^{\mathcal{S}(z_i^b, v^b)} + e^{\mathcal{S}(z_{j>i}^{\neq b}, v^b)}} \quad (2)$$

VIP (Ma et al., 2023b) uses a goal-conditioned approach that separates embeddings of temporally adjacent images while bringing together embeddings of images that are farther apart in time. Given batches of $[I_i, I_{j>i}, I_{j+1}, I_{k \geq j+1}]^{1:B}$, VIP is defined as:

$$\mathcal{L}_{\text{VIP}} = \frac{1-\gamma}{B} \sum_{b \in B} [-\mathcal{S}(z_i^b, z_k^b)] + \log \frac{1}{B} \sum_{b \in B} \exp [\mathcal{S}(z_j^b, z_k^b) + 1 - \gamma \mathcal{S}(z_{j+1}^b, z_k^b)] \quad (3)$$

Just like TCN, we adapt \mathcal{L}_{VIP} to language by replacing $I_{k>h}$ with the embedded language annotation $v = \pi_{\text{text}}(l)$ for the given sequence.

$$\mathcal{L}_{\text{VIP}_{\text{text}}} = \frac{1-\gamma}{B} \sum_{b \in B} [-\mathcal{S}(z_i^b, v^b)] + \log \frac{1}{B} \sum_{b \in B} \exp [\mathcal{S}(z_j^b, v^b) + 1 - \gamma \mathcal{S}(z_{j+1}^b, v^b)] \quad (4)$$

Combinations of these losses reproduce popular reward modeling methods minus regularization terms. R3M is obtained by combining both TCN versions:

$$\mathcal{L}_{\text{R3M}} = \mathcal{L}_{\text{TCN}} + \mathcal{L}_{\text{TCN}_{\text{text}}} \quad (5)$$

Note that R3M adapts TCN to language by training an MLP to predict a similarity score from the concatenated vector $[z_0, z_i, v]$, where z_0 is the first image in the sequence. This approach introduces a non-negligible amount of additional parameters, especially for large embeddings like those from SigLIP2. For fairness, we omit the initial embedding in our setup.

LIV is a combination of both VIP versions plus an InfoNCE objective (Oord et al., 2018), the latter which we also include in our experiments:

$$\mathcal{L}_{\text{LIV}} = \mathcal{L}_{\text{VIP}} + \mathcal{L}_{\text{VIP}_{\text{text}}} + \frac{1}{B} \sum_{b \in B} \left[-\log \frac{e^{\mathcal{S}(z_k^b, v^b)}}{\frac{1}{B} \sum_{j \neq b} e^{\mathcal{S}(z_k^j, v^b)}} \right] \quad (6)$$

Triplet (Schroff et al., 2015) applied to this context reduces the embedding distance between the language goal and the later images of the sequence, and pushes earlier images further away. We propose it as a simple baseline for task progress and show its remarkable effectiveness. Given batches of $[I_i, I_{j>i}, l]^{1:B}$, we use the language annotation as the anchor, the later image as the positive and the earlier image as the negative example. The triplet loss is defined as:

$$\mathcal{L}_{\text{Triplet}} = \sum_{b \in B} \max \left(0, \mathcal{S}(v^b, x_i^b) - \mathcal{S}(v^b, x_j^b) + \alpha \right) \quad (7)$$

where α is the margin controlling how far apart the negative should be from the positive.

3 EXPERIMENTS

3.1 FINETUNING

Learning objectives. We finetune using different configurations of the losses described in 2

$$(1) \mathcal{L}_{\text{Triplet (ours)}} \quad (2) \mathcal{L}_{\text{TCN}_{\text{text}}} \quad (3) \mathcal{L}_{\text{R3M}} \quad (4) \mathcal{L}_{\text{VIP}_{\text{text}}} \quad (5) \mathcal{L}_{\text{VIP}_{\text{text}}} + \mathcal{L}_{\text{VIP}} \quad (6) \mathcal{L}_{\text{LIV}}$$

Model backbone To isolate the performance of the learning objective from model capacity and pre-training, we employ the base version of SigLIP2 (Tschannen et al., 2025) as the backbone for all methods. We finetune using LoRA (Hu et al., 2021) to prevent overfitting.

Data Each model is finetuned on expert demonstrations from the Meta-World environments (Yu et al., 2021). To evaluate out-of-domain performance, we remove 3 tasks from the training data (see 3.2). For the remaining tasks, we collect 3 expert trajectories per task with randomized end-effector initializations, yielding 132 total. To ensure consistent dataset size, we cap the maximum number of samples at 50 thousand and generate them evenly across trajectories. Each timestep is recorded from 3 camera views to enable multi-view training. The timesteps within a sample remain fixed between epochs, but their associated views are randomly reassigned at each iteration, acting as a form of data augmentation to promote view-invariant representations and reduce overfitting.

Implementation details For a complete list of the implementation details, refer to A.1.

3.2 EVALUATION

We wish to learn generalizable reward models which can leverage pre-training knowledge to predict progress on unseen tasks. To this end, we exclude `button-press`, `drawer-open`, and `door-open` environments from the finetuning data and use them for subsequent evaluation metrics. `Button-press` is relatively simple, as success depends mainly on end-effector proximity to a target. In contrast, `drawer-open` and `door-open` are compositional, requiring navigation to the object and subsequent manipulation. Note that we evaluate only the standard `button-press` but remove all its variants to prevent leakage.

To evaluate the performance of finetuned reward models on out-of-domain tasks, we introduce two benchmarks. **(1)** For measuring reward modeling robustness, we collect random and sub-optimal rollouts from each test environment to construct per-task datasets of 10,000 timestep pairs, each labeled by which timestep has the higher ground-truth reward. The model predicts the higher-reward timestep by comparing each element’s similarity to the language goal. Accuracy is defined as the percentage of pairs where this prediction matches the ground-truth ordering. We refer to this benchmark as *consistency with ground-truth reward*. While informative about robustness, this metric does not necessarily indicate that a model can guide an agent towards a goal. **(2)** To evaluate this capacity, we collect 50 expert trajectories per task and predict rewards along each trajectory. Assuming expert timesteps correlate with increasing ground-truth reward, we compute the Value-Order Correlation (VOC) Ma et al. (2024) to measure how well the model’s predicted reward ordering aligns with goal-directed behavior. A model should perform well on both these benchmarks to yield transferable rewards.

4 RESULTS

We report all results on a per-view basis and multi-view. The multi-view is obtained by taking the average similarity scores across views of a timestep, and using it for prediction instead. This evaluates if the objectives were able to take advantage of the multi-view augmentations to learn view-agnostic representations.

Consistency with ground truth reward Table 1 summarizes each model’s task consistency with ground-truth reward accuracy. Triplet loss achieves the highest overall accuracy across all held-out tasks, surpassing both TCN-based and VIP-based objectives. While $\mathcal{L}_{\text{TCN}_{\text{text}}}$ and \mathcal{L}_{R3M} perform similarly, objectives incorporating VIP components exhibit inconsistent ranking ability, often close to random chance. The base SigLIP2 backbone performs slightly below 50%, confirming that finetuning on expert demonstrations is necessary to encode temporal semantics.

Table 1: Consistency with ground truth reward reported as prediction accuracy over random pairs.

	SigLIP2	$\mathcal{L}_{\text{TCN}_{\text{text}}}$	\mathcal{L}_{R3M}	$\mathcal{L}_{\text{VIP}_{\text{text}}}$	$\mathcal{L}_{\text{VIP}_{\text{text}}} + \mathcal{L}_{\text{VIP}}$	\mathcal{L}_{LIV}	$\mathcal{L}_{\text{Triplet (ours)}}$
Button press							
View 1	45.15	69.63	74.42	57.07	57.09	55.29	75.36
View 2	44.81	69.51	71.38	57.09	56.18	54.28	74.15
View 3	44.83	70.27	72.07	56.03	53.69	54.79	74.29
Multi view	40.50	72.24	73.76	57.83	55.31	55.51	76.44
Open drawer							
View 1	42.91	64.52	65.71	65.58	61.76	50.56	69.01
View 2	41.55	61.83	63.25	60.45	59.88	50.77	67.82
View 3	43.60	61.73	61.93	58.49	56.84	49.51	66.33
Multi view	42.13	62.26	62.24	56.43	55.25	47.88	67.01
Open door							
View 1	50.02	64.80	61.04	53.17	49.42	49.28	62.78
View 2	55.04	65.46	62.33	56.80	54.22	50.37	64.27
View 3	54.44	63.98	63.64	58.40	55.04	52.44	64.04
Multi view	57.27	64.96	65.02	60.12	58.57	54.21	65.02
Average	46.85	65.93	66.40	58.12	56.10	52.07	68.88

Alignment with expert progress As shown in Table 2, VOC scores reveal a similar trend. The triplet objective demonstrates strong correlations with expert progress, surpassing VIP based objectives on all tasks and rivaling TCN based objectives on `button-press` and `drawer-open`. In contrast, VIP based objectives exhibit high variance and frequent negative correlations even on the easier `button-press`, indicating reward inconsistencies along expert trajectories. All methods collapse on `door-open`, indicating a need for methods more adapted to multi-step tasks. Overall, these findings still support the conclusion that simpler ranking-based losses are capable of producing accurate and robust reward models. See A.4 for visualizations of predicted reward over expert trajectories for each model.

Table 2: Alignment with expert progress reported as VOC scores (percentage).

	SigLIP2	$\mathcal{L}_{\text{TCN}_{\text{text}}}$	\mathcal{L}_{R3M}	$\mathcal{L}_{\text{VIP}_{\text{text}}}$	$\mathcal{L}_{\text{VIP}_{\text{text}}} + \mathcal{L}_{\text{VIP}}$	\mathcal{L}_{LIV}	$\mathcal{L}_{\text{Triplet (ours)}}$
Button press							
View 1	-72.80 \pm 10.87	89.08 \pm 5.80	81.78 \pm 2.78	27.39 \pm 24.04	-21.03 \pm 13.11	16.67 \pm 17.89	95.47 \pm 2.11
View 2	-19.50 \pm 17.28	90.92 \pm 3.43	90.95 \pm 2.98	54.95 \pm 16.77	56.60 \pm 19.61	40.71 \pm 24.08	90.03 \pm 3.28
View 3	-11.51 \pm 17.60	82.55 \pm 5.20	79.10 \pm 4.04	77.94 \pm 9.55	63.89 \pm 9.89	32.12 \pm 16.22	81.72 \pm 3.27
Multi view	-56.30 \pm 13.40	94.53 \pm 2.41	86.87 \pm 2.81	68.21 \pm 15.57	56.72 \pm 14.08	42.9 \pm 15.35	95.07 \pm 2.29
Open drawer							
View 1	-56.76 \pm 29.20	82.17 \pm 5.21	87.70 \pm 3.90	65.68 \pm 8.22	54.28 \pm 14.35	61.99 \pm 6.56	87.67 \pm 3.90
View 2	-29.86 \pm 24.33	80.92 \pm 4.89	83.71 \pm 4.75	69.87 \pm 17.17	53.92 \pm 31.42	66.99 \pm 10.04	76.94 \pm 4.26
View 3	19.7 \pm 28.93	75.88 \pm 12.34	80.88 \pm 7.01	67.54 \pm 13.45	64.17 \pm 12.27	55.47 \pm 16.78	86.76 \pm 4.12
Multi view	-28.84 \pm 37.83	86.14 \pm 2.80	87.22 \pm 3.25	77.59 \pm 9.53	75.17 \pm 9.33	80.40 \pm 5.39	90.17 \pm 2.26
Open door							
View 1	-14.8 \pm 20.33	-42.27 \pm 15.58	2.21 \pm 22.80	-25.8 \pm 12.50	-0.04 \pm 17.66	17.51 \pm 17.43	26.01 \pm 26.31
View 2	7.84 \pm 18.36	42.66 \pm 23.50	7.7 \pm 17.50	-33.03 \pm 15.55	-15.03 \pm 15.53	-5.99 \pm 14.20	22.11 \pm 22.34
View 3	29.52 \pm 17.17	31.43 \pm 21.83	33.7 \pm 23.65	-30.36 \pm 14.86	-27.62 \pm 13.04	-0.28 \pm 10.80	-7.01 \pm 16.21
Multi view	11.82 \pm 17.89	10.40 \pm 17.69	14.33 \pm 20.68	-31.39 \pm 13.38	-18.94 \pm 11.91	-0.64 \pm 10.23	6.70 \pm 17.91
Average	-18.46 \pm 21.10	60.36 \pm 10.06	61.35 \pm 9.68	32.38 \pm 14.22	28.51 \pm 15.18	33.99 \pm 13.75	62.64 \pm 9.02

5 CONCLUSION & FUTURE WORK

In this work, we revisit the learning objectives of recent vision-language reward models and evaluate them under a unified framework controlling for architecture, data, and training conditions. We find that a simple triplet loss can outperform more complex objectives in robustness to sub-optimal trajectories, and that ranking-based objectives correlate more strongly with ground-truth rewards. These results underscore the need for standardized benchmarks for fair and consistent evaluation. Future work includes deeper analysis of each objective to understand their failure cases, scaling to larger datasets, more challenging multi-step tasks, and temporal compression methods.

REFERENCES

- Dima Damen, Hazel Doughty, Giovanni Maria Farinella, Sanja Fidler, Antonino Furnari, Evangelos Kazakos, Davide Moltisanti, Jonathan Munro, Toby Perrett, Will Price, and Michael Wray. Scaling egocentric vision: The epic-kitchens dataset, 2018. URL <https://arxiv.org/abs/1804.02748>.
- Jacob Devlin, Ming-Wei Chang, Kenton Lee, and Kristina Toutanova. Bert: Pre-training of deep bidirectional transformers for language understanding, 2019. URL <https://arxiv.org/abs/1810.04805>.
- Kristen Grauman, Andrew Westbury, Eugene Byrne, Zachary Chavis, Antonino Furnari, Rohit Girdhar, Jackson Hamburger, Hao Jiang, Miao Liu, Xingyu Liu, Miguel Martin, Tushar Nagarajan, Ilija Radosavovic, Santhosh Kumar Ramakrishnan, Fiona Ryan, Jayant Sharma, Michael Wray, Mengmeng Xu, Eric Zhongcong Xu, Chen Zhao, Siddhant Bansal, Dhruv Batra, Vincent Cartillier, Sean Crane, Tien Do, Morrie Doulaty, Akshay Erapalli, Christoph Feichtenhofer, Adriano Fragomeni, Qichen Fu, Abraham Gebreselasie, Cristina Gonzalez, James Hillis, Xuhua Huang, Yifei Huang, Wenqi Jia, Weslie Khoo, Jachym Kolar, Satwik Kottur, Anurag Kumar, Federico Landini, Chao Li, Yanghao Li, Zhenqiang Li, Karttikeya Mangalam, Raghava Modhugu, Jonathan Munro, Tullie Murrell, Takumi Nishiyasu, Will Price, Paola Ruiz Puentes, Meray Ramazanova, Leda Sari, Kiran Somasundaram, Audrey Southerland, Yusuke Sugano, Ruijie Tao, Minh Vo, Yuchen Wang, Xindi Wu, Takuma Yagi, Ziwei Zhao, Yunyi Zhu, Pablo Arbelaez, David Crandall, Dima Damen, Giovanni Maria Farinella, Christian Fuegen, Bernard Ghanem, Vamsi Krishna Ithapu, C. V. Jawahar, Hanbyul Joo, Kris Kitani, Haizhou Li, Richard Newcombe, Aude Oliva, Hyun Soo Park, James M. Rehg, Yoichi Sato, Jianbo Shi, Mike Zheng Shou, Antonio Torralba, Lorenzo Torresani, Mingfei Yan, and Jitendra Malik. Ego4d: Around the world in 3,000 hours of egocentric video, 2022. URL <https://arxiv.org/abs/2110.07058>.
- Edward J. Hu, Yelong Shen, Phillip Wallis, Zeyuan Allen-Zhu, Yuanzhi Li, Shean Wang, Lu Wang, and Weizhu Chen. Lora: Low-rank adaptation of large language models, 2021. URL <https://arxiv.org/abs/2106.09685>.
- Siddharth Karamcheti, Suraj Nair, Annie S. Chen, Thomas Kollar, Chelsea Finn, Dorsa Sadigh, and Percy Liang. Language-driven representation learning for robotics, 2023. URL <https://arxiv.org/abs/2302.12766>.
- Yecheng Jason Ma, William Liang, Vaidehi Som, Vikash Kumar, Amy Zhang, Osbert Bastani, and Dinesh Jayaraman. Liv: Language-image representations and rewards for robotic control, 2023a. URL <https://arxiv.org/abs/2306.00958>.
- Yecheng Jason Ma, Shagun Sodhani, Dinesh Jayaraman, Osbert Bastani, Vikash Kumar, and Amy Zhang. Vip: Towards universal visual reward and representation via value-implicit pre-training, 2023b. URL <https://arxiv.org/abs/2210.00030>.
- Yecheng Jason Ma, Joey Hejna, Ayzaan Wahid, Chuyuan Fu, Dhruv Shah, Jacky Liang, Zhuo Xu, Sean Kirmani, Peng Xu, Danny Driess, Ted Xiao, Jonathan Tompson, Osbert Bastani, Dinesh Jayaraman, Wenhao Yu, Tingnan Zhang, Dorsa Sadigh, and Fei Xia. Vision language models are in-context value learners, 2024. URL <https://arxiv.org/abs/2411.04549>.
- Suraj Nair, Aravind Rajeswaran, Vikash Kumar, Chelsea Finn, and Abhinav Gupta. R3m: A universal visual representation for robot manipulation, 2022. URL <https://arxiv.org/abs/2203.12601>.
- Aaron van den Oord, Yazhe Li, and Oriol Vinyals. Representation learning with contrastive predictive coding. *arXiv preprint arXiv:1807.03748*, 2018.
- Simone Parisi, Aravind Rajeswaran, Senthil Purushwalkam, and Abhinav Gupta. The unsurprising effectiveness of pre-trained vision models for control, 2022. URL <https://arxiv.org/abs/2203.03580>.
- Alec Radford, Jong Wook Kim, Chris Hallacy, Aditya Ramesh, Gabriel Goh, Sandhini Agarwal, Girish Sastry, Amanda Askell, Pamela Mishkin, Jack Clark, Gretchen Krueger, and Ilya Sutskever. Learning transferable visual models from natural language supervision, 2021. URL <https://arxiv.org/abs/2103.00020>.

- Juan Rocamonde, Victoriano Montesinos, Elvis Nava, Ethan Perez, and David Lindner. Vision-language models are zero-shot reward models for reinforcement learning, 2024. URL <https://arxiv.org/abs/2310.12921>.
- Olga Russakovsky, Jia Deng, Hao Su, Jonathan Krause, Sanjeev Satheesh, Sean Ma, Zhiheng Huang, Andrej Karpathy, Aditya Khosla, Michael Bernstein, Alexander C. Berg, and Li Fei-Fei. Imagenet large scale visual recognition challenge, 2015. URL <https://arxiv.org/abs/1409.0575>.
- Florian Schroff, Dmitry Kalenichenko, and James Philbin. Facenet: A unified embedding for face recognition and clustering. In *2015 IEEE Conference on Computer Vision and Pattern Recognition (CVPR)*, pp. 815–823. IEEE, June 2015. doi: 10.1109/cvpr.2015.7298682. URL <http://dx.doi.org/10.1109/CVPR.2015.7298682>.
- Pierre Sermanet, Corey Lynch, Yevgen Chebotar, Jasmine Hsu, Eric Jang, Stefan Schaal, and Sergey Levine. Time-contrastive networks: Self-supervised learning from video, 2018. URL <https://arxiv.org/abs/1704.06888>.
- Michael Tschannen, Alexey Gritsenko, Xiao Wang, Muhammad Ferjad Naeem, Ibrahim Alabdulmohsin, Nikhil Parthasarathy, Talfan Evans, Lucas Beyer, Ye Xia, Basil Mustafa, Olivier Hénaff, Jeremiah Harmsen, Andreas Steiner, and Xiaohua Zhai. Siglip 2: Multilingual vision-language encoders with improved semantic understanding, localization, and dense features, 2025. URL <https://arxiv.org/abs/2502.14786>.
- Tianhe Yu, Deirdre Quillen, Zhanpeng He, Ryan Julian, Avnish Narayan, Hayden Shively, Adithya Bellathur, Karol Hausman, Chelsea Finn, and Sergey Levine. Meta-world: A benchmark and evaluation for multi-task and meta reinforcement learning, 2021. URL <https://arxiv.org/abs/1910.10897>.

A APPENDIX

A.1 HYPERPARAMETERS

Note that LIV objectives suffered from instability and required a learning rate of $1e - 5$ to get meaningful results.

Table 3: Training hyperparameters for the SigLIP-LoRA model.

Parameter	Symbol	Value
Total samples	N_{samples}	5×10^4
Validation split	r_{val}	0.1
LoRA rank	r	16
LoRA alpha	α_l	32
Epochs	T	5
Batch size	B	32
Learning rate	η	1×10^{-4}
Minimum learning rate	η_{min}	1×10^{-6}
Scheduler	–	Cosine Annealing
Margin (triplet)	α	0.3
Negatives (all methods)	–	3

A.2 EXAMPLE OF DIFFERENT VIEWS IN METAWORLD

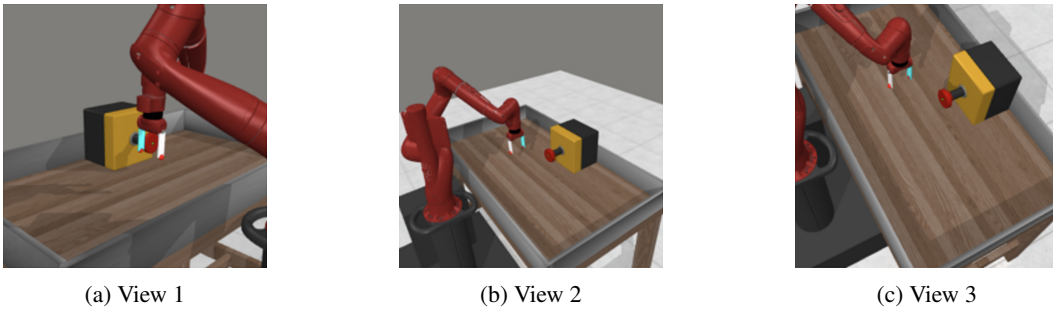


Figure 1: The button-press environment seen from all 3 views. This example illustrates the occlusion problem often encountered in robotics, highlighting the importance of multi-view training and spatial planning.

A.3 LANGUAGE GOAL

Table 4: Language descriptions of the goal for all Metaworld tasks used in our experiments. Underlined tasks are left out the training set, and bold tasks are used for out-of-domain testing.

Task	Description
assembly-v3	pick up a nut and place it onto a peg
basketball-v3	dunk the basketball into the basket
bin-picking-v3	grasp the green object from its bin and place it into the other bin
box-close-v3	grasp the cover and close the box with it
<u>button-press-topdown-v3</u>	press the button on the box
<u>button-press-topdown-wall-v3</u>	bypass the wall and press the button on the box
button-press-v3	press the button
<u>button-press-wall-v3</u>	bypass the wall and press the button
<u>coffee-button-v3</u>	push the button on the coffee machine
dial-turn-v3	rotate the dial 180 degrees
disassemble-v3	pick the nut out of a peg
door-close-v3	close the door with a revolving joint
door-lock-v3	lock the door by rotating the lock clockwise
door-open-v3	open the door with a revolving joint
<u>door-unlock-v3</u>	unlock the door by rotating the lock counter-clockwise
hand-insert-v3	insert the gripper into the hole
faucet-open-v3	turn on faucet
faucet-close-v3	turn off faucet
hammer-v3	hammer the screw on the wall
handle-press-side-v3	press the handle down
handle-press-v3	press the handle down
handle-pull-side-v3	pull the handle up
handle-pull-v3	pull the handle up
lever-pull-v3	pull the lever down 90 degrees
pick-place-wall-v3	pick the red object, bypass the wall and place the object on the target
pick-out-of-hole-v3	pick up the object from the hole
pick-place-v3	pick and place the red object to the goal
plate-slide-v3	slide the puck into the hockey net
plate-slide-side-v3	slide the puck into the hockey net
plate-slide-back-v3	get the puck from the hockey net
plate-slide-back-side-v3	get the puck from the hockey net
peg-insert-side-v3	insert the peg in the hole
peg-unplug-side-v3	unplug the peg from the hole
soccer-v3	kick the soccer ball into the goal
stick-push-v3	grasp the blue stick and push the box using the stick
stick-pull-v3	grasp the blue stick and pull the box using the stick
push-v3	push the red object to the green objective
push-wall-v3	bypass the wall and push the object behind the wall
push-back-v3	push the red object back to the green objective
reach-v3	reach the red goal position
reach-wall-v3	bypass the wall and reach the red goal position
shelf-place-v3	pick up the blue object and place it onto the shelf
sweep-into-v3	sweep the object into the hole
sweep-v3	sweep the object off the table
window-open-v3	open the window using the handle
window-close-v3	close the window using the handle
drawer-close-v3	close the green drawer
drawer-open-v3	open the green drawer
<u>coffee-push-v3</u>	push the mug to the red goal under the coffee machine
<u>coffee-pull-v3</u>	pull the mug to the green goal

A.4 REWARD OVER EXPERT TRAJECTORIES

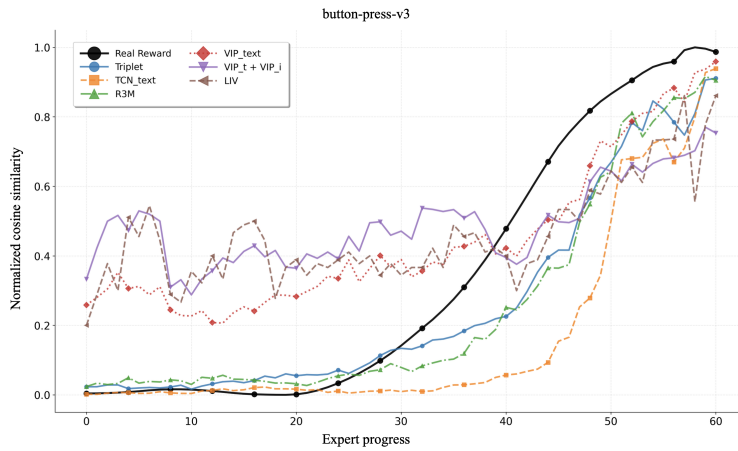


Figure 2: Progression of the reward generated by each model over an expert trajectory in the button-press-v3 environment.

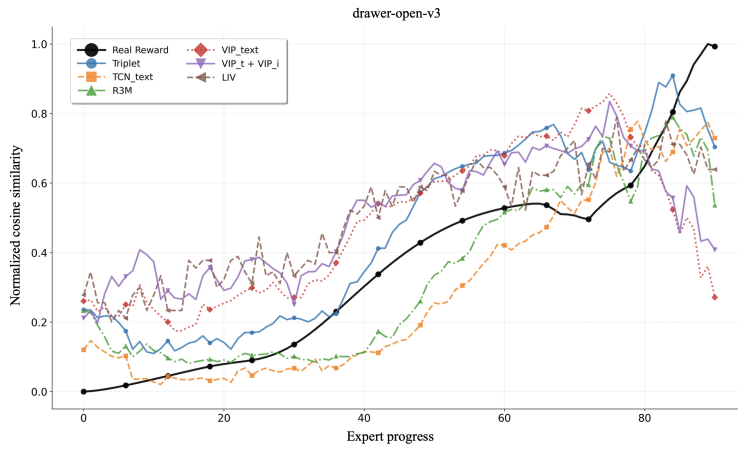


Figure 3: Progression of the reward generated by each model over an expert trajectory in the drawer-open-v3 environment.

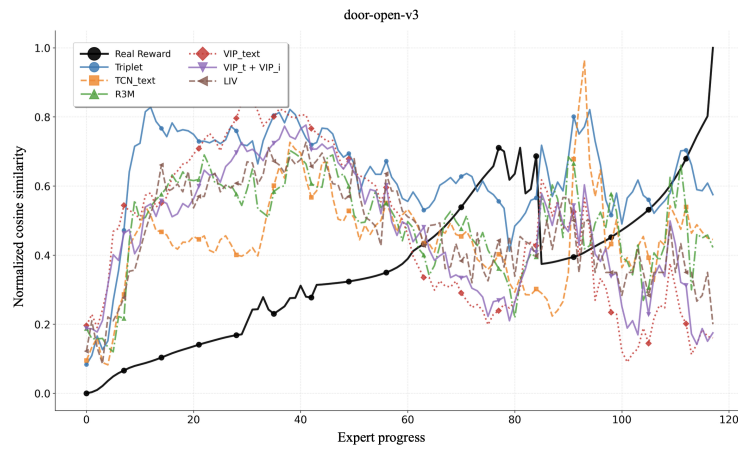


Figure 4: Progression of the reward generated by each model over an expert trajectory in the door-open-v3 environment.